Revision 2

Thermo-elastic behaviour of grossular garnet at high pressures and temperatures

S. Milani[1], R.J. Angel[1], L. Scandolo[2], M.L. Mazzucchelli[2], T. Boffa Ballaran[3], S. Klemme[4], M.C. Domeneghetti[2], R. Miletich[5], K. S. Scheidl[5], M. Derzsi[1,6], K. Tokár[7], M. Prencipe[8], M. Alvaro[2], F. Nestola[1]

[1]Department of Geosciences, University of Padova, Via Gradenigo, 6, I-35131 Padova, Italy
[2]Department of Earth and Environmental Sciences, University of Pavia, Via A. Ferrata, 1, I-27100 Pavia, Italy
[3]Bayerisches Geoinstitut, Universität Bayreuth, 95440 Bayreuth, Germany
[4]Institut für Mineralogie, Westfälische Wilhelms-Universität Münster, Corrensstraße 24 – 48149 Münster, Germany
[5]Institut für Mineralogie und Kristallographie, Universität Wien, Althanstrasse 14, A-1090 Wien, Austria
[6]Centre for New Technologies, University of Warsaw, Żwirki i Wigury 93, 02089 Warsaw, Poland
[7]Institute of Physics, CCMS, Slovak Academy of Sciences, Dúbravská cesta 9, 84511 Bratislava, Slovakia
[8]Department of Earth Sciences, Via Valperga Caluso 35, I-10125 Turin, Italy

For submission to: American Mineralogist
Running title: P-V-T-K fit on grossular

ABSTRACT

The thermo-elastic behaviour of synthetic single crystals of grossular garnet ($Ca_3Al_2Si_3O_{12}$) has been studied *in situ* as a function of pressure and temperature separately. The same data collection protocol has been adopted to collect both the pressure-volume (*P*-*V*) and temperature-volume (*T*-*V*) datasets in order to make the measurements consistent with one another. The consistency between the two datasets allows simultaneous fitting to a single pressure-volume-temperature equation of state (EoS), which was performed with a new fitting utility implemented in the latest version of the program EoSFit7c. The new utility performs fully weighted *simultaneous* fits of the *P*-*V*-*T* and *P*-*K*-*T* data using a thermal pressure Equation of State combined with any PV EoS. Simultaneous refinement of our *P*-*V*-*T* data combined with that of K^T as a function of *T* allowed us to produce a single *P*-*V*-*T*-K^T equation of state with the following coefficients:

V_0 = 1664.46(5) Å^3, K_{T0} = 166.57(17) GPa and $K`$ = 4.96(7) $\alpha_{(300K,\ 1bar)}$ = 2.09(2)*10^{-5} K^{-1} with a refined Einstein temperature (θ_E) of 512K for a Holland-Powell-type thermal pressure model and a Tait 3rd-order EoS. Additionally, thermodynamic properties of grossular have been calculated for the first time from crystal Helmholtz and Gibbs energies, including the contribution from phonons, using density functional theory within the framework of the quasi-harmonic approximation.

Keywords: grossular, high-pressure, high-temperature, diffraction, bulk modulus, P-V-T-K fit, EosFit

This is a preprint, the final version is subject to change, of the American Mineralogist (MSA)
Cite as Authors (Year) Title. American Mineralogist, in press.
DOI: https://doi.org/10.2138/am-2017-5855

1. INTRODUCTION

Stable over a wide range of pressure and temperature conditions, garnets are among the most abundant phases in the Earth's upper mantle and transition zone. Yet coherent and homogeneous equation of state coefficients to reliably describe their behaviour at simultaneous high pressures and temperatures still have to be determined with high accuracy and precision. Recent papers have shown the importance of a robust and valid description of the elastic behaviour of the most abundant mineral phases for the accurate calculation of host-inclusion entrapment pressures that in turn allow the growth conditions in the Earth to be inferred (e.g. Angel et al. 2014, 2015a, 2015b; Ashley et al. 2015; Milani et al. 2015). However, the determination of a full set of elastic coefficients of a mineral is always challenging because of the limitations in performing simultaneous high-pressure (P) and temperature (T) experiments on one side and because of the lack of consistent measurements performed separately at high-P and high-T. Therefore, a reliable description of the elastic behaviour of minerals at high-P,T with a single set of Equation of State (EoS) coefficients can be extremely challenging.

Pressure-volume EoS are well-developed and are capable of reproducing the isothermal volume or density changes of materials to within the experimental uncertainties. A natural approach to describing the P-V-T behaviour of a material is therefore to describe how the volume (V_{0T}), bulk moduli (K_{0T}[1]) and its pressure derivatives (K_{0T}') change with increasing temperature (at room pressure), and then use these parameters to calculate the isothermal compression at the temperature of interest. A potential limitation of this approach is that while the variation of K_{0T} with T can be measured, the variation of K_{0T}' with T has been measured very rarely, although it is obvious that it should increase slightly with increasing temperature. As Helffrich and Connolly (2009) pointed out,

[1] Notation: subscripts on K (e.g. $K_{P,T}$) indicate the reference pressure and temperature to which the bulk modulus is referred; superscripts S or T (e.g. K^S or K^T) stand for adiabatic or isothermal quantities.

This is a preprint, the final version is subject to change, of the American Mineralogist (MSA)
Cite as Authors (Year) Title. American Mineralogist, in press.
DOI: https://doi.org/10.2138/am-2017-5855

the common assumption that K_{0T}' does not change with temperature in combination with the approximation that $\partial K_{0T}/\partial T$ is constant, often leads to the prediction of non-physical negative thermal expansion coefficients at reasonably modest pressures for a large number of materials. An alternative approach is to employ the idea of thermal pressure (e.g. Anderson 1995). Then the total pressure (P) at a given V and T can be expressed as the sum of two terms:

$$P(V,T) = P(V,T_{ref}) + Pth(T)$$

The function $P(V,T_{ref})$ is the isothermal equation of state for material at the reference temperature, up to the volume at P and T_{ref}. As shown in the Figure 1, if $T > T_{\mathrm{ref}}$, then $P(V,T_{ref}) < P(V,T)$. The thermal-pressure $Pth(T)$ is the pressure that would be created by increasing the temperature from T_{ref} to T at constant volume, which is the isochor of the material passing through the final P,T point of interest. As shown in Figure 1, the concept of thermal pressure is therefore essentially a way of calculating $P(V,T)$ along a different path in P-T space. We can consider that the isothermal compression part that gives us $P(V,T_{ref})$ is well-defined. The slope of the isochor is given by $\left(\frac{\partial P}{\partial T}\right)_V = \frac{\alpha}{\beta} = \alpha K^T$ (where α is the volume thermal expansion and β is the compressibility of the material) so the thermal pressure is $Pth = \int_{Tref}^{T} \left(\alpha K^T\right)_V dT$. In order to use a thermal-pressure EoS one then has to know, or to make an assumption, about how the product αK^T varies along the isochor. For many materials and P,T ranges of interest (e.g. Figure 1) the temperatures are in the region of the Debye temperature, so the isochor is linear and thus αK_T is a constant. In this case $Pth \sim \left(\alpha K^T\right)_V (T - Tref)$.

A number of other assumptions or models of the behaviour of the material can be made, including the Debye and similar models which make assumptions about the vibrational and hence thermal behaviour of materials. Holland and Powell (2011) noted that the form of αK^T against

This is a preprint, the final version is subject to change, of the American Mineralogist (MSA)
Cite as Authors (Year) Title. American Mineralogist, in press.
DOI: https://doi.org/10.2138/am-2017-5855

temperature should have the shape of a heat capacity function and developed an approximation for the integral of αK^T that involves an Einstein function, as follows:

$$Pth = \alpha_0 K_{00} \left(\frac{\theta_E}{\xi_0} \right) \left(\frac{1}{\exp\left(\theta_E / T\right) - 1} - \frac{1}{\exp\left(\theta_E / T_{ref}\right) - 1} \right)$$

with ξ_0 being the same as in the thermal expansion equation of Kroll et al. (2012). This thermal-pressure model has the physically-correct properties that the product αK^T becomes constant at high temperatures while it decreases to zero at low temperatures. This means that both the bulk modulus K_{0T} and the thermal expansion become constant at low temperatures, and both have an approximately linear variation with temperature above θ_E. The exact expressions for thermal expansion and bulk modulus as a function of temperature depend on the choice of isothermal equation of state, but at T_{ref} and zero pressure $\alpha = \alpha_0$ (Holland and Powell 2011). In this study we used the Holland and Powell (2011) model of thermal pressure in combination with the Tait isothermal EoS (so as to maintain compatibility with Thermocalc, Holland and Powell 2011) to determine the EoS of grossular ($Ca_3Al_2Si_3O_{12}$) garnet. We show that the thermal pressure approach allows the full *P*-*V*-*T* EoS to be determined by fitting simultaneously measurements of the volume and bulk modulus over a range of temperature but only at room pressure. Additional separate measurements of the volume compression curve at high-*P* can be used to provide either an independent test of the EoS parameters, or be used to further constrain them in simultaneous global fits of all available data. This approach has the advantage of not requiring data from simultaneous high-*P*, high-T measurements which remain challenging with respect to both the control and accurate measurement of *P* and *T*, and with respect to the precision in volume measurements. A comparison with previous literature data (e.g. Skinner 1956; Isaak et al. 1992; Thieblot et al. 1998; Kono et al. 2010; Gwanmesia et al. 2014; Du et al. 2015 etc..) is provided together with a further crosscheck of our experimental data against the results obtained by density functional theory (DFT) ab-initio simulation. Thermodynamic properties of grossular have been calculated for the first time

from crystal Helmholtz and Gibbs energies, including the contribution from phonons, using density functional theory within the framework of the quasi-harmonic approximation.

2. METHODS

2.1 Sample synthesis and characterization

Synthetic single crystals of pure end-member grossular (Gr_{100}) garnets were synthesized at high pressures with a multi-anvil apparatus at the Bayerisches Geoinstitut. Stoichiometric mixtures of CaO (prepared by decarbonation of $CaCO_3$), $Al(OH)_3$ and SiO_2 were packed into platinum capsules of 3.5 mm length and 2 mm diameter. Samples were synthesized at 6 GPa and 1300°C. The experimental sample was heated in 23 mins and the temperature was kept at 1300°C for 40 mins. Each multi-anvil experiment was performed with Cr-doped MgO octahedra of 18 mm edge length combined with tungsten carbide cubes of 11 mm truncation-edge lengths. For all the experiments a graphite heater was employed. Experiments were quenched by cutting the electrical power supply to the furnace. Single-crystals of up to ca. 100 μm in diameter were recovered from the capsules. The compositions of the crystals have been determined by electron microprobe at the University of Padova using a Cameca CAMEBAX-micro operating at 15 nA and 15 kV with standards of andradite for Si, spinel for Al and diopside for Ca. Results from the chemical analyses are reported in Table 1. Two crystals (with size ca. 80 x 30 x 30 μm) were selected for the X-ray diffraction study based on the absence of twinning and visible inclusions and on the quality of their diffraction peak profiles (FWHM not greater than 0.15°). The synthesized grossular garnets were confirmed to contain negligible amounts of H_2O. FTIR analyses were performed on the crystals and show OH absorption bands consistent with approximately 5 ppm of H_2O.

147 *2.2 Thermal expansion behaviour by single crystal X-ray diffraction experiments*

148 The high-temperature single-crystal X-ray diffraction experiments were performed at the
149 University of Pavia with a HUBER four-circle point detector diffractometer operating at 50 kV and
150 30 mA (Mo$K\alpha$ radiation) and equipped with a 0.8 mm short collimator and automated with the
151 SINGLE software (Angel and Finger 2011). This diffractometer is equipped with a newly designed
152 micro-furnace controlled by a Eurotherm temperature regulator (Alvaro et al. 2015). For the high-*T*
153 experiments, one single crystal of grossular was placed inside a thin-walled quartz vial (0.3 mm
154 inner diameter and 26 mm long) and held in position by means of quartz wool. The vial was then
155 mounted on a metal goniometer head on the diffractometer. During the high-temperature
156 experiments the effects of the crystal offsets and the diffractometer aberrations were compensated
157 by using the eight-position centring method (King and Finger 1979) before starting the high-*T*
158 measurement. The unit-cell parameters (Table 2 and Figure 2) were determined at 23 different
159 temperatures from room-*T* up to 1020 K using only 4-position centring because of the spatial
160 restrictions described in Alvaro et al. (2015). A further 7 measurements were then made on cooling
161 back to room temperature. Each individual measurement took about 12 hours, and the high-
162 temperature experiment lasted for a total of 14 days. Unconstrained unit-cell parameters confirmed
163 the cubic symmetry within 1 e.s.d. Therefore, only constrained unit-cell parameters obtained by
164 vector least-squares fit (Ralph and Finger 1982) are reported in Table 2. Unit-cell parameters
165 determined on the heating and cooling cycles are indistinguishable.

166 The low-temperature single-crystal X-ray diffraction experiment was performed on the very
167 same crystal used for the high-T experiment still mounted inside its quartz vial. The experiment was
168 carried out at the Institut für Mineralogie und Kristallographie at the University of Wien using a
169 Stoe StadiVari diffractometer equipped with an Incoatec IμS microsource (Mo-target, with multi-
170 layer mirror optics, operating at 50kV and 0.1mA) and a Pilatus 300K area detector. Low
171 temperatures were achieved using an Oxford Cryojet system that allows measurements to be
172 performed between 100 and 500 K. Full intensity data collections up to 110° 2θ (with a coverage of

99% and redundancy higher than 4) were performed at 10 different temperatures from room-*T* down to 100 K. Correction of the crystal offsets from the goniometer center were made by first performing a short data collection and adjusting the crystal position to make the frame scale factors flat. Unconstrained unit-cell parameters confirmed the cubic symmetry within 1 e.s.d.; therefore, only constrained unit-cell parameters are reported in Table 2 and Figure 2 together with those obtained at high-*T*.

2.3 Compressibility behaviour by single crystal X-ray diffraction experiments

High-pressure single-crystal X-ray diffraction experiments for the grossular garnet were carried out with a Huber four-circle diffractometer at the Bayerisches Geoinstitut. The diffractometer operates at 50 kV and 40 mA (MoKα radiation), is equipped with a point detector and is automated by SINGLE software (Angel and Finger 2011). The sample was loaded in a ETH-type diamond-anvil cell (DAC, Miletich et al. 2000) using a steel gasket, pre-indented to 100 μm thickness and with a hole diameter of 250 μm. Methanol:ethanol mixture 4:1 was used as pressure transmitting medium, which remains hydrostatic up to about ~ 9.5 GPa (Angel et al. 2007; Klotz et al. 2009). A single crystal of quartz was loaded in the DAC together with the sample and used as a pressure standard (Angel et al. 1997). During the centring procedure, the effects of crystal offsets and diffractometer aberrations were eliminated from the refined peak position by the eight-position centring method (King and Finger 1979). Unconstrained unit-cell parameters were obtained by vector least-squares fit (Ralph and Finger 1982) on not less than 20 reflections up to $2\theta = 29°$. The symmetry-unconstrained unit-cell edges show deviations smaller than 1 e.s.d. from the constrained ones thus confirming the cubic symmetry within 1 e.s.d.. Therefore, only the constrained unit-cell parameters have been reported in Table 3 and Figure 3.

2.4 Fitting of the pressure-volume-temperature-modulus data using EoSFit7c

This is a preprint, the final version is subject to change, of the American Mineralogist (MSA)
Cite as Authors (Year) Title. American Mineralogist, in press.
DOI: https://doi.org/10.2138/am-2017-5855

P-V-T-K fit on grossular

All fits described in this manuscript have been performed with the EosFit7c program (Angel et al. 2014). Previous versions of this program were able to fit isothermal EoS, thermal expansion models and the thermal-pressure EoS of Holland and Powell (2011) to *P*-*V*, *V*-*T* or *P*-*V*-*T* data, by the method of least-squares. We have now extended the capabilities of EosFit-7c to also fit all of these forms of EoS to bulk and linear moduli, either alone or in combination with volume or unit-cell parameter data. Fits are performed by weighted non-linear least squares to minimise the residuals P_{obs}-P_{calc}, using the effective variance method (Orear 1982) to convert the experimental uncertainties in volume and bulk moduli, pressure and temperature of each datum into an effective uncertainty in *P* (Angel 2000). Input bulk moduli can be either adiabatic (K^S) or isothermal values (K^T), but in either case they must be Reuss values, corresponding to the response of the material under hydrostatic pressure. The Voigt and Reuss bulk moduli of a material quantify its volume response to the application of uniform strain and uniform stress (hydrostatic pressure) respectively. When uniform stress is applied to a cubic material, it undergoes isotropic (i.e. uniform) strain. Therefore, the Voigt and Reuss bulk moduli of a cubic material are identical. We remind the reader that this is not true for materials of lower symmetry and therefore the use of Voigt values, or Voigt-Reuss-Hill averages, in Equations of state of crystals with symmetry lower than cubic is inconsistent with the theory underlying equations of state under hydrostatic conditions, and will lead to incorrect results (e.g. Angel et al. 2009).

If the input moduli to EosFit7c are isothermal, no further conversion is made, and the observational equations for such data in the least-squares are simply the expression for the bulk modulus in terms of pressure for each EoS. These expressions are direct for invertible EoS such as the Murnaghan or Tait EoS (Freund and Ingalls 1989; Holland and Powell 2011; Angel et al. 2014). For non-invertible EoS the procedure used is to calculate the compression ratio V/V_{00} corresponding to the observed *K* and then use the *P*-*V* expression of the EoS to calculate the corresponding pressure. If adiabatic moduli are provided as input data, they are converted to isothermal values by $K^S = (1+\alpha_V \gamma T)K^T$ where the value of thermal expansion (α_V) is taken from the current EoS at the

This is a preprint, the final version is subject to change, of the American Mineralogist (MSA)
Cite as Authors (Year) Title. American Mineralogist, in press.
DOI: https://doi.org/10.2138/am-2017-5855

pressure and temperature of interest. The Grüneisen parameter γ can be expressed in terms of measurable quantities, for example $\gamma = \frac{\alpha_V K^S}{C_p} = \frac{\alpha_V K^T}{C_V}$. However, since heat capacity data is not available at elevated pressures, in EosFit7c we use the simple approximation (Anderson 1996) that $\gamma(P,T) = \gamma_0\left(\frac{V(P,T))}{V_0}\right)^q$, with the value of q close to 1 for 'normal' solids under modest P,T conditions. Only Boehler and Ramakrishnan (1980) and Boehler (1982) appear to have attempted to measure the value of q, showing that it scales with volume. This means that the Grüneisen parameter scales with volume, increasing with increasing temperature and decreasing upon compression, which when considered as a measure of the pressure-dependence of the frequencies of vibrational modes, is reasonable. This will break down when the material becomes very anharmonic, near to structural phase transitions, but should not be a problem for materials such as the grossular garnet in this study. The value of γ_0 (i.e. γ value at the reference conditions) and of q can be set by the user in Eosfit7c.

For linear moduli that describe the variation of the unit-cell parameters with pressure as $M_i^T = -a_i \frac{\partial P}{\partial a_i}$, the procedure is analogous to that used for linear dimensions in EosFit7 (Angel et al., 2014). Internally the linear moduli are converted to volume-like bulk moduli as $K_i = \frac{M_i}{3}$ and treated with volume EoS. For the conversion of adiabatic to linear moduli, we use the relationship between isothermal and adiabatic compressibilities $\beta_i^T = \beta_i^S + \frac{\alpha_i \alpha_V T}{C_p}$ which can be derived from the fundamental relationship between isothermal and adiabatic elastic compliances $s_{ijkl}^T = s_{ijkl}^S + \frac{\alpha_{ij}\alpha_{kl}T}{C_p}$ with the C_p in units of $Jm^{-3}K^{-1}$ (Nye 1985). The substitution $\frac{\gamma}{K^S} = \frac{\alpha_V}{C_p}$ gives $\beta_i^T = \beta_i^S + \frac{\alpha_i \gamma T}{K^S} = \beta_i^S\left(1 + \frac{\alpha_i \gamma T \beta_V^S}{\beta_i^S}\right)$ which can be rewritten in terms of moduli as

244 $M_i^S = \left(1 + \alpha_i \gamma T \frac{M_i^S}{K^S}\right) M_i^T$. It is important to notice that for cubic materials $\alpha_i = \alpha_V / 3$ and $\frac{M_i^S}{K^S} = 3$

245 so that only for cubic materials this can be written as $M^S = (1 + \alpha_v \gamma T) M^T$ which is the same

246 relation as for the bulk moduli.

247

248 *2.5 Ab-initio DFT (Density Functional Theory)*

249 Ab-initio calculations have been performed in order to crosscheck our experimental results at
250 simultaneous high-*P* and *T*. Thermodynamic properties of grossular have been calculated from
251 crystal Helmholtz and Gibbs energies, including the contribution from phonons, using density
252 functional theory (DFT) within the framework of the quasi-harmonic approximation (QHA).
253 Periodic DFT calculations were performed with the plane-wave VASP package (Kresse and
254 Furthmüller 1996) within the PBE-GGA approximation (Perdew et al. 1996), with projector-
255 augmented waves (PAW, Blöchl 1994) and the PBEsol functional (Perdew et al. 2008). A plane-
256 wave cutoff of 520 eV (1.3 x default VASP value) was used as recommended in the VASP package.
257 Energy convergence was tested for two k-meshes 2x2x2 and 4x4x4. Since the denser mesh did not
258 lead to any significant reduction in energy ($\Delta E < 0.001$ eV) the 2x2x2 mesh was used both for unit cell
259 optimization and subsequent calculation of interatomic forces. The cell was optimized at 17
260 pressure points within the range [-8 to 8GPa] with step of 1 GPa. The threshold for electronic and
261 ionic convergence was set to 10^{-8} and 10^{-6} eV, respectively. The atomic forces were converged to
262 10^{-5} eV/Å. Phonon frequencies at constant cell volumes were calculated in program PHONOPY
263 (Togo and Tanaka 2015) which takes advantage of the direct method of Parlinsky et al. (1997). The
264 force constants used to construct the dynamical matrices (input for PHONOPY) were calculated in
265 the VASP package using density functional perturbation theory (DFPT, Baroni et al. 2001) and
266 taking into account symmetries of the conventional body-centered cell of the garnet, containing 160
267 atoms. The results obtained with PBE-GGA commonly overestimate cell volume values of ionic
268 solids by up to 9.5% with respect to experimental results while PBEsol functional brings the

discrepancy down to 2% (Perdew et al. 2008). In our case, the DFT calculations yielded volume values of 1664.6 Å^3 (static DFT), 1681.9 Å^3 (zero-point vibration included) and 1687.3 Å^3 (T=290 K) which agree with experimental values of 1664.3 Å at room *P* and *T*, (0.0001 GPa and 300 K) within 0.0 %, 1.1% and 1.4% respectively. This volume overestimation amounts to about -2 GPa, on the pressure scale, with respect to the experimental datum.

3. RESULTS

3.1 Temperature-volume data

The room-*PT* unit-cell volumes (V_{00}) of grossular as determined in this study, agree with one another to better than 1 e.s.d. thus confirming the reliability of the unit-cell lattice determination with different instruments and measurement protocols. Therefore, we combined the high-*T* measurements together with those at low-*T* in a single dataset without any normalization or re-scaling. The evolution of the unit-cell volume with temperature is reported in Figure 2 and Table 2 where the low-*T* and the high-*T* data are reported together. A continuous increase of the unit-cell volume is observed as a function of temperature with no evidence of any irreversible change in the crystal occurred up to the maximum temperature reached in this study. Data collected both with increasing and decreasing temperature overlap within experimental error, thus indicating good experimental reproducibility. The temperature-volume data for the entire range of *T* studied were fit using the software EoSFit7c (Angel et al. 2014) using a Kroll-type EoS (Kroll et al. 2012) allowing for refinement of the Einstein temperature (θ_E) but not refining K′ value that was kept fixed to 5 (i.e. the value from compressibility data, see the following sections). The thermal expansion coefficients obtained were $\alpha_{(298K,\ 1bar)}$ = 2.08(2)*10^{-5} K^{-1}, V_{00} = 1664.45(7) Å^3 with θ_E= 515(20) K. We compared our *T*-*V* for grossular with those from Isaak (1992) determined by dilatometry. Isaak et al. (1992) measured physical expansions, and converted such values to volume expansions Yv(obs). Conversion of Isaak et al. (1992) data (taken from their Table 2) to unit-cell volumes has been performed according to $V = V_0(1 + Y_V obs)$. In order to ensure that our measurements and those

This is a preprint, the final version is subject to change, of the American Mineralogist (MSA)
Cite as Authors (Year) Title. American Mineralogist, in press.
DOI: https://doi.org/10.2138/am-2017-5855

by Isaak et al. (1992) were on the same volume scale we used our V_{00} at the same reference temperature of 293K used by Isaak et al. (1992). A plot of the two datasets (see Figure 2) shows that they agree within their mutual uncertainties.

3.2 Temperature-volume-bulk modulus data

Isaak et al. (1992) also determined the adiabatic bulk modulus of grossular by RUS measurements and then used measured heat capacity data and their own thermal expansion data to also calculate the isothermal bulk modulus at each measurement temperature by means of $K^S = (1+\alpha_V \gamma T)K^T$, using the value of the Grüneisen parameter $\gamma = \frac{\alpha_V K^S}{C_p}$. The reliability of the heat capacity (C_p) data by Isaak et al. (1992) has been confirmed by comparison with the more recent data by Bosenick et al. (1996) (see Figure 4). The C_p values determined by Isaak et al. (1992) fall well within the scatter of the data determined by Bosenick et al. (1996) and are also in good agreement with those we have obtained from the DFT calculations.

Using K and V data as a function of T it is obviously possible to refine V_{00}, α_0, θ_E and K_{00} . But in addition it is possible and required to refine K' because this affects the results when using the thermal pressure model as it appears in the isothermal EoS $P(V,T_{ref})$, and at room pressure $P(V,T_{ref}) = -Pth(T)$. Simultaneous refinement of our T-V data and the T-K^S data from Isaak et al. (1992) for grossular using γ_0=1.22 and q=0 (i.e. γ=γ0) yielded identical results as to those obtained from fitting the T-V-K^T data (see Table 4[2]). This shows that the assumption that γ is constant is a reasonable approximation for grossular. This observation is also in agreement with Isaak et al. (1992) who calculated that γ drops by 0.1(± 0.05) over the temperature range from 300K to 1200K and with our results from DFT calculations as shown in Figure 4 according to which γ drops to 1.24

[2] The Equation of State coefficients reported in Table 4c representing the best fit of our data have been deposited as supplementary material in the form of .eos files (that can be read with EoSFit7c). They are also available directly from the authors.

317 at 650K and then it assumes constant values (e.g. changes of about 2 at the 3rd decimal place) above
318 650K.
319
320 *3.3 Pressure-volume data*
321 The unit-cell volume decreases smoothly with increasing pressure, as shown in Figure 3 and
322 reported in Table 2, up to the maximum hydrostatic pressure reached in this study of ~7.5 GPa.
323 Such pressure covers the stability pressure range for upper mantle garnets. Fit of the *P-V* data alone
324 using a 3rd order Tait EoS yielded the following coefficients: V_{00} = 1664.36(7) Å^3, K_{00} =
325 167.45(1.04) GPa and K_{00}` = 4.93(31) also reported in Table 4a. The goodness of the fit results was
326 confirmed by the low ΔP_{max} value (calculated as $|P_{obs} - P_{calc}|$) of 0.010 GPa. The equation of state
327 coefficients obtained with this method agree with those obtained by *T-V-K* fitting to better than 1
328 e.s.d. thus confirming the reliability of the results from the two fitting approaches.
329
330 *3.4 P-V-T-K and PVT Equation of State*
331 The remarkably good agreement between the lattice parameters as determined with different
332 experimental settings and that of the EoS coefficients obtained with different procedures allowed us
333 to perform a simultaneous refinement of the entire set of EoS coefficients by combining our
334 pressure-volume and temperature-volume data together with those of temperature-bulk modulus
335 (Isaak et al. 1992) into a single dataset. Fully weighted simultaneous fit of the *P-V-T-K* data has
336 been performed using a thermal pressure Equation of State with a 3rd order Tait EoS, allowing
337 simultaneous refinement of V_{00}, K_{00}, K_{00}', α_0 and θ_E. As expected, the resulting coefficients V_{00} =
338 1664.46(5) Å^3; K_{00}=166.57(17) GPa; K_{00}'=4.96(7); $\alpha_{(298K,\ 1bar)}$ = 2.09(2)*10^{-5} K^{-1}, with θ_E= 512(19)K
339 (γ_0=γ=1.22) agree within 2 σ to those from *P-V* and *T-V-K* separately (see Table 4). At this point it
340 is important to point out that the main difference between the *P-V-T-K* and *T-V-K* fits can be seen in
341 the description of the bulk moduli as a function of *T* (Figure 5a). It should be clear from Figure 5a
342 that while in the thermal regime between room-*T* and the maximum temperature reached with the

experiments the bulk moduli calculated from the *T-V-K* and *P-V-T-K* Equations of State agree within mutual uncertainties, in the low-*T* regime much larger discrepancies are observed. These discrepancies are due to the different values of θ_E in the two EoS.

Simultaneous refinement of the *P-V-T* data alone yielded the following coefficients V_{00} = 1664.44(6) Å^3; K_{00}=166.19(1.25) GPa; K_{00}'=5.14(40); $\alpha_{(298K,\ 1bar)}$ = 2.09(2)*10^{-5} K^{-1}, with θ_E= 512K (not refined). Standard deviations on the bulk modulus (K_{0T}) and its first derivative (K') obtained from the *P-V-T* fitting are 6-8 times larger than those from the *P-V-T-K* ones and, when considered, the resulting coefficients from the *P-V-T* fit agree within 1 sigma with those obtained from the *P-V-T-K* fits. The *P-V-T* results are not showed in Figure 5a for sake of clarity, however, the resulting bulk moduli as a function of *T* agrees with the experimental data within 1 σ.

4. DISCUSSION

4.1 Thermal expansion: comparison with literature data

The measured room temperature-pressure volumes (V_{00}) reported in this study are in good agreement with those previously reported in literature by several authors (see Table 4a and b). So far, only few X-ray diffraction thermal expansion data are available for grossular garnet (e.g. Skinner 1956; Bosenick and Geiger 1997; Thieblot et al. 1998; Du et al. 2015) and most of them have been obtained by means of powder X-ray diffraction. Data from Du et al. (2015) and those by Skinner (1956) have been re-fitted to their entire temperature range 296 K - 859 K (excluding two outliers at 393 K and 477 K) and 284 K -980 K, respectively. On the other hand, data from Thieblot et al. (1998) have been fitted from 300 K to 1453 K (i.e. well below the decomposition temperature) excluding a few outliers at 607 K, 724 K, and 1241 K. The results of all the extrapolations at 300 K are reported in Table 4b and shown Figure 2. As shown in Table 4b, there are considerable differences between our data and those available in literature. These can be most likely ascribed to the compositional differences between the various samples and/or to the uncertainties given by the different experimental methods. For example, both Skinner (1956) and Thieblot et al. (1998) used grossular-rich samples for their investigation. For sake of comparison, regardless the compositional

This is a preprint, the final version is subject to change, of the American Mineralogist (MSA)
Cite as Authors (Year) Title. American Mineralogist, in press.
DOI: https://doi.org/10.2138/am-2017-5855

differences, these literature data have been re-fitted to Fei-type EoS (Fei 1995). Results from the fitting are reported in Table 4b, and Figure 2.

As shown in Figure 2, our data for the low-*T* regime are in good agreement with those reported by Bosenick and Geiger (1997) if their most scattered data (e.g. 195, 220 and 295 K) are not considered.

The thermal expansion coefficients at 300 K from both Skinner (1956) and Du et al. (2015) are smaller than those calculated from our fitting. The discrepancies between our dataset and that by Skinner (1956) could be ascribed to the differences in composition as their sample referred to as a 'grossularite' has not been properly characterized. The thermal coefficient value obtained fitting the data by Du et al. (2015) is not reliable as demonstrated by the negative thermal expansion at high-*T* (regardless of the Equation of State model chosen). The same is true also for the data reported by Thieblot et al. (1998), where the thermal expansion value decreases with increasing temperature. Our datasets, ranging from 100 K to about 1000 K, allowed fitting of a Kroll-type EoS (Kroll et al. 2012), leading to a much more reliable description of the thermal behaviour of grossular. The reliability of the Einstein temperatures used (θ_E=569(13) K) have been confirmed by comparison with the saturation temperature (where $T_{sat} \approx \theta_E/2$) obtained from the fitting of the low-*T* data alone (T_{sat}=270(6) K) using a Salje-type EoS (Salje et al. 1991). The agreement within 1 sigma is also achieved when comparing with the θ_E from the *P-V-T-K* fit [θ_E=512(19) K, see Table 4c]

4.2 Compressibility: comparison with literature data

The elastic coefficients for grossular have been determined in several studies using different methods (e.g. ultrasonic wave velocity, static compression experiments in diamond-anvil cell, ab-initio calculations) as summarised in Table 4a. For purpose of comparison with the literature data, the adiabatic bulk modulii (K^S) obtained by means of ultrasonic wave velocity techniques have been converted to K^T.

394 DFT calculations of a P(V) curve, fitted by a third order Birch-Murnaghan EoS, provide a
395 value of 156 GPa for the bulk modulus K^T at 300K, and a K′ of 4.22. The *static* (no zero point and
396 thermal effects included) and the *athermal* (zero point corrected and a temperature of 0K) values
397 are respectively 163.9 and 160.1 GPa (K′ fixed at 4.22: the value we obtained at 300K). These
398 results are in line with the *standard* performances of DFT-GGA Hamiltonians like PBEsol, as they
399 generally underestimate bulk moduli by about 10 GPa at room temperature. Another DFT study
400 from the literature (Erba et al. 2014) provided a somewhat higher bulk modulus (171 GPa), but that
401 was a result from a static calculation with a hybrid HF/DFT (B3LYP) Hamiltonian which includes
402 an Hartree-Fock correction to the DFT-GGA electronic exchange functional. Indeed, such
403 correction proved to be crucial to compute bulk moduli (and vibrational frequencies) very close to
404 the experimental data (Prencipe et al. 2009, 2011, 2012, 2014), but it is computationally very costly
405 if a plane-wave basis set is used, as in the present case, and therefore it cannot be afforded. The
406 largest discrepancy in grossular bulk modulus value is with respect to the results obtained by Kawai
407 and Tsuchiya (2012) with a lattice dynamics approach together in combination with a LDA
408 functional. Furthermore, the first derivative of the bulk modulus (K′) which we could now reliably
409 refine clearly demonstrates that the correct value must be very close to 5 in agreement with some of
410 the previous studies (see Table 4a).
411
412 *4.3 Full elastic behaviour (P-V-T-K): comparison with literature data*
413 The new utility available in EoSFit7c allowed us to also apply the same method described in
414 the sections above (*P-V-T-K* fitting) to the available literature data obtained from independent
415 elastic measurements and *PVT* datasets (Kono et al. 2010; Gwanmesia et al. 2014). It is remarkable
416 the extra constraint given by the simultaneous weighted fit of the *K* data (see results in Table 4c)
417 which however applied to the literature dataset does not allow to obtain the same quality as for our
418 elastic coefficients due to the lack of data in the low-temperature regime. This combined with the
419 much lower accuracy and precision that in most cases arises by the limitation of the *P-V-T*

This is a preprint, the final version is subject to change, of the American Mineralogist (MSA)
Cite as Authors (Year) Title. American Mineralogist, in press.
DOI: https://doi.org/10.2138/am-2017-5855

simultaneous measurements (i.e. pressure calibrant, pressure transmitting media etc.) give rise to discrepancies such as those showed in Figure 5b. In this case the discrepancies in bulk modulus values at high-*T* reach up to 4% (more than 6 GPa at 1400 K). In order to crosscheck the measurements with the DFT results, we performed fitting of the DFT data in the temperature range between 400 and 800K using a thermal pressure equation of state combined with a 3rd order Tait-eos. For purpose of comparison with the other fits, bulk moduli values have been normalized to the bulk moduli extrapolated at 0K from the P-V-T-K fit of the experimental data (Fig. 5a, red line). The trend of the two fits agrees within 1σ thus confirming the reliability of our fitting results via P-V-T-K fits even at the highest temperature where the DFT approach leads to the smallest deviations from the experimental data.

4. CONCLUSIONS AND IMPLICATIONS

It is obvious that pressure-volume or temperature-volume measurements alone do not provide strong constraints on the cross-terms in *P-T* space (e.g. $\partial K/\partial T$ or $\partial \alpha/\partial P$) which are fundamental for the description of the elastic properties of a material at simultaneous high-*P* and high-*T*. Limitation in experimental measurements and/or in the description of the pressure-volume-temperature data (e.g. incorrect Equations of State, erroneous mis-use of Voigt, Reuss isothermal or adiabatic bulk moduli) has often in the past lead to inaccurate unreliable or even completely wrong results (e.g. negative thermal expansion, erroneous $\partial K/\partial T$ etc…) specially when the EoS are subsequently extrapolated to high-*P,T*.

Pressure-volume EoS are well-developed and, if correctly used, are capable of reproducing the isothermal volume or density changes of materials to within the experimental uncertainties. Previous versions of the EoSFit program were able to fit isothermal EoS, thermal expansion models and the thermal-pressure (Holland and Powell 2011) to *P-V*, *V-T* or *P-V-T* data, by the method of least-squares. We have now extended the capabilities of EosFit7c to also fit all of these forms of EoS to bulk and linear moduli, either alone or in combination with volume or unit-cell parameter data. With this approach we can now provide a reliable description of the variation of *K′* with *T* thus

avoiding mistaken extrapolations leading to non-physical behaviour as often occurs for several materials (Helffrich and Connolly 2009).

The consistency of the results obtained with this new fitting procedure has been shown by comparison of results from using adiabatic and isothermal moduli. It has also been demonstrated the importance of performing fitting with this procedure in terms of both accuracy and precision of the thermoelastic coefficients when the *PT* cross-terms ($\partial K/\partial T$ or $\partial \alpha/\partial P$) are extrapolated in *PT* space (see Figure 5b). Additionally, thermodynamic functions were calculated for grossular using DFT approach within QHA. The obtained results are in fairly good agreement with experiment, when allowing for the known short-comings of the functionals employed in the DFT.

Acknowledgment

This work has been supported by the ERC Starting Grant (n° 307322) to F. Nestola. MA has been supported by the SIR-MIUR grant MILE DEEp (n° RBSI140351) to M. Alvaro. MD acknowledges computational grant G62-24 at Interdisciplinary Centre for Mathematical and Computational Modelling (ICM) of the University of Warsaw. RM and KSS acknowledge support through grant BE532003 of the University of Vienna. We thank Tom Duffy (Princeton) for advice and discussions. We would also like to thank R. Carampin (IGGCNR, Padova) for help with the electron microprobe analyses. We thank Andrea D'Alpaos and Mario Putti (University of Padova) for advice on least-squares minimisation.

REFERENCES

Alvaro, M., Angel, R.J., Marciano, C., Milani, S., Scandolo, L., Mazzucchelli, M.L., Zaffiro, G., Rustioni, G., Briccola, M., Domeneghetti, M.C., and others (2015) A new micro-furnace for in situ high-temperature single-crystal X-ray diffraction measurements. Journal of Applied Crystallography, 48, 1192–1200.

Anderson, D.L. (1995) Equations of State of Solids for Geophysics and Ceramic Science. Oxford University Press. Oxford, UK.

Anderson, O.L. (1996) Anharmonicity of forsterite and the thermal pressure of insulators.

Geophysical Research Letters, 23, 3031–3034.

Angel, R.J. (2000) Equations of state. In R.M. Hazen and R.T. Downs, Eds., Reviews in Mineralogy: High temperature and high pressure crystal chemistry. Mineralogical Society of America, Washington, D.C.

Angel, R.J., and Finger, L.W. (2011) SINGLE: a program to control single-crystal diffractometers. Journal of Applied Crystallography, 44, 247–251.

Angel, R.J., Allan, D.R., Milletich, R., and Finger, L.W. (1997) The use of quartz as an internal pressure standard in high-pressure crystallography. Journal of Applied Crystallography, 30, 461–466.

Angel, R.J., Bujak, M., Zhao, J., Gatta, G.D., and Jacobsen, S.D. (2007) Effective hydrostatic limits of pressure media for high-pressure crystallographic studies. Journal of Applied Crystallography, 40, 26–32.

Angel, R.J., Jackson, J.M., Reichmann, H.J., and Speziale, S. (2009) Elasticity measurements on minerals: a review. European Journal of Mineralogy, 21, 525–550.

Angel, R.J., Gonzalez-Platas, J., and Alvaro, M. (2014) EosFit7c and a Fortran module (library) for equation of state calculations. Zeitschrift fur Kristallographie, 229, 405–419.

Angel, R.J., Nimis, P., Mazzucchelli, M.L., Alvaro, M., and Nestola, F. (2015a) How large are departures from lithostatic pressure? Constraints from host-inclusion elasticity. Journal of Metamorphic Geology, 33, 801–813.

Angel, R.J., Alvaro, M., Nestola, F., and Mazzucchelli, M.L. (2015b) Diamond thermoelastic properties and implications for determining the pressure of formation of diamond-inclusion systems. Russian Geology and Geophysics, 56, 211-220.

Ashley, K.T., Darling, R.S., Bodnar, R.J., and Law, R.D. (2015) Significance of "stretched" mineral inclusions for reconstructing P–T exhumation history. Contributions to Mineralogy and Petrology, 169, 1–9.

Baroni, S., De Gironcoli, S., Dal Corso, A., and Giannozzi, P. (2001) Phonons and related crystal

503 properties from density-functional perturbation theory. Reviews of Modern Physics, 73, 515–
504 562.
505 Blöchl, P.E. (1994) Projector augmented-wave method. Physical Review B, 50, 17953–17979.
506 Boehler, R. (1982) Adiabats of quartz, coesite, olivine, and magnesium oxide to 50 kbar and 1000
507 K, and the adiabatic gradient in the Earth's mantle. Journal of Geophysical Research: Solid
508 Earth, 87, 5501–5506.
509 Boehler, R., and Ramakrishnan, J. (1980) Experimental results on the pressure dependence of the
510 Gruneisen parameter: a review. Journal of Geophysical Research, 85, 6996–7002.
511 Bosenick, A., and Geiger, C.A. (1997) Powder X ray diffraction study of synthetic pyrope-grossular
512 garnets between 20 and 295 K. Journal of Geophysical Research-All Series, 102, 22.
513 Bosenick, A., Geiger, C.A., and Cemič, L. (1996) Heat capacity measurements of synthetic pyrope-
514 grossular garnets between 320 and 1000 K by differential scanning calorimetry. Geochimica et
515 Cosmochimica Acta, 60, 3215–3227.
516 Du, W., Clark, S.M., and Walker, D. (2015) Thermo-compression of pyrope-grossular garnet solid
517 solutions: Non-linear compositional dependence. American Mineralogist, 100, 215–222.
518 Erba, A., Mahmoud, A., Orlando, R., and Dovesi, R. (2014) Elastic properties of six silicate garnet
519 end members from accurate ab initio simulations. Physics and Chemistry of Minerals, 41, 151–
520 160.
521 Fei, Y. (1995) Thermal Expansion. In Mineral Physics & Crystallography: A Handbook of Physical
522 Constants pp. 29–44. American Geophysical Union.
523 Freund, J., and Ingalls, R. (1989) Inverted isothermal equations of state and determination of B0,
524 B'0 and B0. Journal of Physics and Chemistry of Solids, 50, 263–268.
525 Gwanmesia, G.D., Wang, L., Heady, A., and Liebermann, R.C. (2014) Elasticity and sound
526 velocities of polycrystalline grossular garnet (Ca3Al2Si3O12) at simultaneous high pressures
527 and high temperatures. Physics of the Earth and Planetary Interiors, 228, 80–87.
528 Helffrich, G., and Connolly, J.A.D. (2009) Physical contradictions and remedies using simple

529 polythermal equations of state. American Mineralogist, 94, 1616–1619.
530 Holland, T.J.B., and Powell, R. (2011) An improved and extended internally consistent
531 thermodynamic dataset for phases of petrological interest, involving a new equation of state for
532 solids. Journal of Metamorphic Geology, 29, 333–383.
533 Isaak, D.G., Anderson, O.L., and Oda, H. (1992) High-temperature thermal expansion and elasticity
534 of calcium-rich garnets. Physics and Chemistry of Minerals, 19, 106–120.
535 Kawai, K., and Tsuchiya, T. (2012) First principles investigations on the elasticity and phase
536 stability of grossular garnet. Journal of Geophysical Research: Solid Earth, 117, 1–8.
537 King, H.E., and Finger, L.W. (1979) Diffracted Beam Crystal Centering and Its Application to
538 High-Pressure Crystallography. Journal of Applied Crystallography, 12, 374–378.
539 Klotz, S., Chervin, J.C., Munsch, P., and Marchand, G. Le (2009) Hydrostatic limits of 11 pressure
540 transmitting media. Journal of Physics D: Applied Physics, 42, 75413.
541 Kono, Y., Gréaux, S., Higo, Y., Ohfuji, H., and Irifune, T. (2010) Pressure and temperature
542 dependences of elastic properties of grossular garnet up to 17 GPa and 1 650 K. Journal of
543 Earth Science, 21, 782–791.
544 Kresse, G., and Furthmüller, J. (1996) Efficient iterative schemes for ab initio total-energy
545 calculations using a plane-wave basis set. Physical Review B, 54, 11169–11186.
546 Kroll, H., Kirfel, A., Heinemann, R., and Barbier, B. (2012) Volume thermal expansion and related
547 thermophysical parameters in the Mg, Fe olivine solid-solution series. European Journal of
548 Mineralogy, 24, 935–956.
549 Milani, S., Nestola, F., Alvaro, M., Pasqual, D., Mazzucchelli, M.L., Domeneghetti, M.C., and
550 Geiger, C.A. (2015) Diamond-garnet geobarometry: The role of garnet compressibility and
551 expansivity. Lithos, 227, 140–147.
552 Miletich, R., Allan, D.R., and Kuhs, W.F. (2000) High-pressure single-crystal techniques. High-
553 Temperature and High-Pressure Crystal Chemistry, 41, 445–519.
554 Nye, J.F. (1985) Physical Properties of Cristals: Their Representation by Tensors and Matrices.

555 Oxford University Press.
556 Orear, J. (1982) Least squares when both variables have uncertainties. American Journal of Physics,
557 50, 912.
558 Parlinski, K., Li, Z., and Kawazoe, Y. (1997) First-Principles Determination of the Soft Mode in
559 Cubic ZrO2. Physical Review Letters, 78, 4063–4066.
560 Perdew, J., Ruzsinszky, A., Csonka, G., Vydrov, O., Scuseria, G., Constantin, L., Zhou, X., and
561 Burke, K. (2008) Restoring the Density-Gradient Expansion for Exchange in Solids and
562 Surfaces. Physical Review Letters, 100, 136406.
563 Perdew, J.P., Burke, K., and Ernzerhof, M. (1996) Generalized Gradient Approximation Made
564 Simple. Physical Review Letters, 77, 3865–3868.
565 Prencipe, M., Noel, Y., Bruno, M., and Dovesi, R. (2009) The vibrational spectrum of lizardite-1T
566 [Mg3Si 2O5(OH)4] at the Γ point: A contribution from an ab initio periodic B3LYP
567 calculation. American Mineralogist, 94, 986–994.
568 Prencipe, M., Scanavino, I., Nestola, F., Merlini, M., Civalleri, B., Bruno, M., and Dovesi, R.
569 (2011) High-pressure thermo-elastic properties of beryl (Al4Be6Si12O36) from ab initio
570 calculations, and observations about the source of thermal expansion. Physics and Chemistry
571 of Minerals, 38, 223–239.
572 Prencipe, M., Mantovani, L., Tribaudino, M., Bersani, D., and Lottici, P.P. (2012) The Raman
573 spectrum of diopside: a comparison between ab initio calculated and experimentally measured
574 frequencies. European Journal of Mineralogy, 24, 457–464.
575 Prencipe, M., Bruno, M., Nestola, F., De La Pierre, M., and Nimis, P. (2014) Toward an accurate ab
576 initio estimation of compressibility and thermal expansion of diamond in the [0, 3000 K]
577 temperature and [0, 30 GPa] pressures ranges, at the hybrid HF/DFT theoretical level.
578 American Mineralogist, 99, 1147–1154.
579 Ralph, R.L., and Finger, L.W. (1982) A Computer-Program for Refinement of Crystal Orientation
580 Matrix and Lattice-Constants from Diffractometer Data with Lattice Symmetry Constraints.

Journal of Applied Crystallography, 15, 537–539.

Salje, E.K.H., Wruck, B., and Thomas, H. (1991) Order-parameter saturation and low-temperature extension of Landau theory. Zeitschrift für Physik B Condensed Matter, 82, 399–404.

Skinner, B.J. (1956) Physical properties of end-members of the garnet group. American Mineralogist, 41, 428–436.

Thieblot, L., Roux, J., and Richet, P. (1998) High-temperature thermal expansion and decomposition of garnets. European Journal of Mineralogy, 10, 7.

Togo, A., and Tanaka, I. (2015) First principles phonon calculations in materials science. Scripta Materialia, 108, 1–5.

Figure captions

Figure 1. Figure illustrating the two ways to calculate P-V-T properties.

Figure 2. Unit-cell volume and thermal expansion. In all graphs black solid lines represent fitting results obtained on our data using the P-V-T-K approach and black dashed line those obtained from the T-V-K approach. The error bars are smaller than symbol size. (a) our data (solid symbol) together with the available low-T literature data (empty symbols); (b) Only the high-T regime (i.e. above room-T) for our data (solid symbol) together with the available high-T literature data (empty symbols); (c) Volume thermal expansion coefficient as a function of temperature obtained from the fitting of our data using P-V-T-K (solid line) and T-V-K (dashed line) fitting approach.

Figure 3. Pressure-volume data for grossular available in literature (open symbols) together with the data from this study (filled symbols). The dashed line represents the fitting of our data to a 3rd – order Tait EoS. The error bars are smaller than the symbol size.

Figure 4. (a) Heat capacity (C_p) values used in this work as determined by Isaak (1992) compared with the recent data by Bosenick and Geiger (1996). Also data obtained from DFT calculations are shown with the red solid line. (b) Gruneisen parameter as a function of temperature for different pressures as obtained from the DFT calculations.

Figure 5. Bulk modulus evolution with temperature. (a) Isothermal (K_T, filled symbols) and adiabatic (K_s, empty symbols) bulk moduli from Isaak (1992) together with those from T-V-K (dotted line) and P-T-V-K (solid line) fitting of our data. The red line corresponds to the bulk moduli obtained from fitting the DFT results using a thermal pressure combined with a 3rd order Tait EoS as described in the text. (b) normalized experimental isothermal bulk modulus (K_T, solid symbols) together with the extrapolation of our fitting results (obtained from P-T-V-K fit, solid line) and those obtained with the same method from the data from Kono et al. (2010) and Gwanmesia et al. (2014) (dashed and dotted line, respectively). The agreement between our data extrapolated at high-T and the experimental data by Isaak (1992) is remarkable; whereas large differences occurs between our data and those obtained with the same fitting approach from the data by Kono et al (2010) and Gwanmesia et al. (2014).

This is a preprint, the final version is subject to change, of the American Mineralogist (MSA)
Cite as Authors (Year) Title. American Mineralogist, in press.
DOI: https://doi.org/10.2138/am-2017-5855

Figure 1

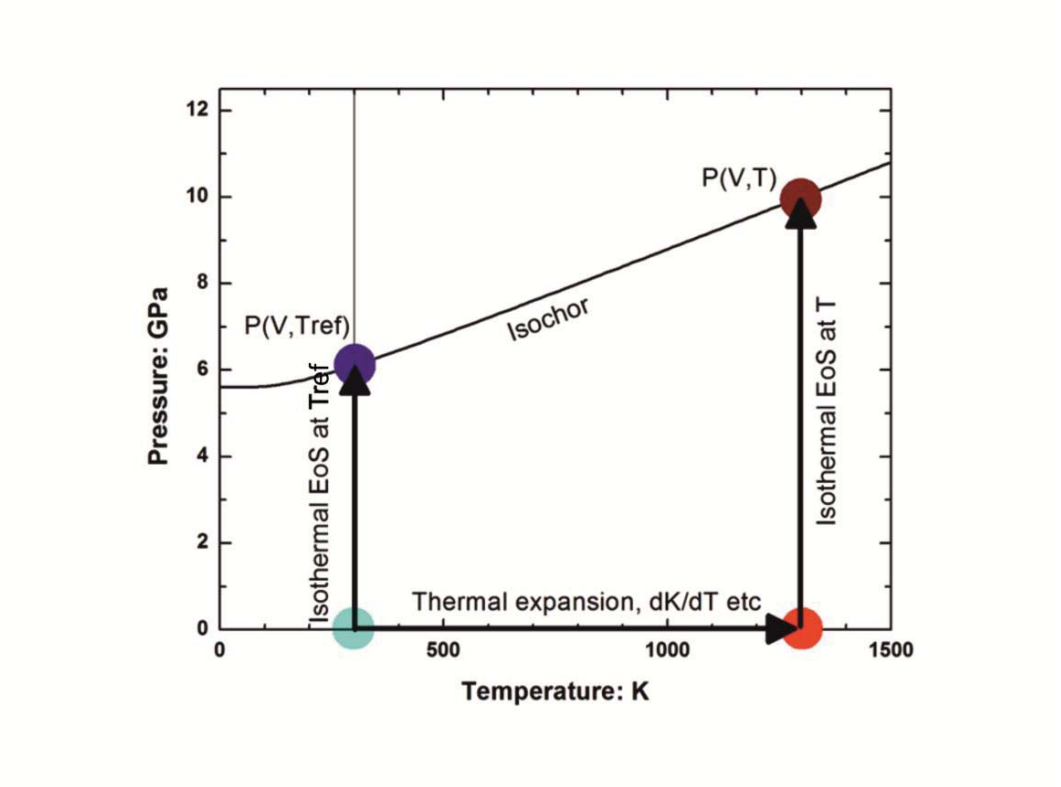

This is a preprint, the final version is subject to change, of the American Mineralogist (MSA)
Cite as Authors (Year) Title. American Mineralogist, in press.
DOI: https://doi.org/10.2138/am-2017-5855

Figure 2A

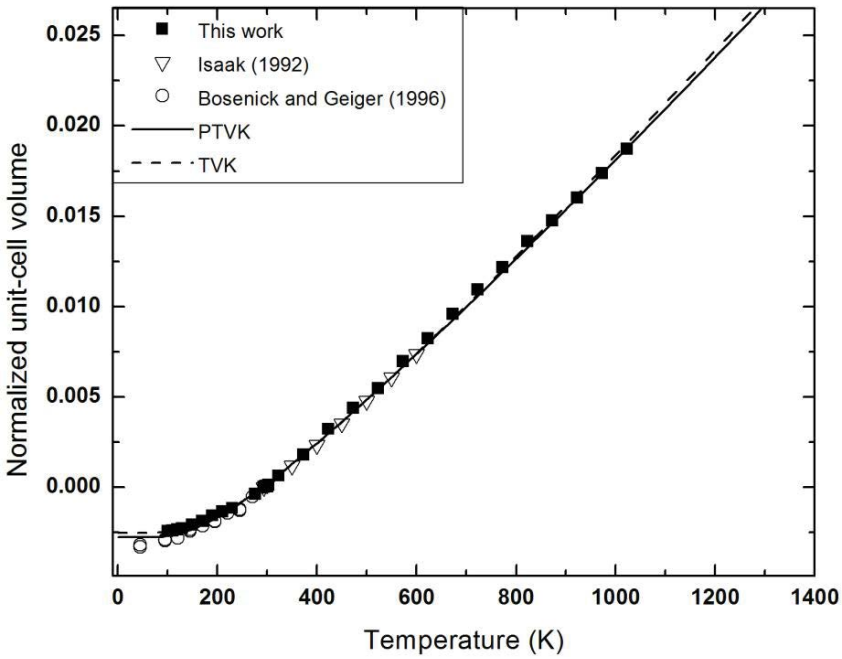

This is a preprint, the final version is subject to change, of the American Mineralogist (MSA)
Cite as Authors (Year) Title. American Mineralogist, in press.
DOI: https://doi.org/10.2138/am-2017-5855

Figure 2B

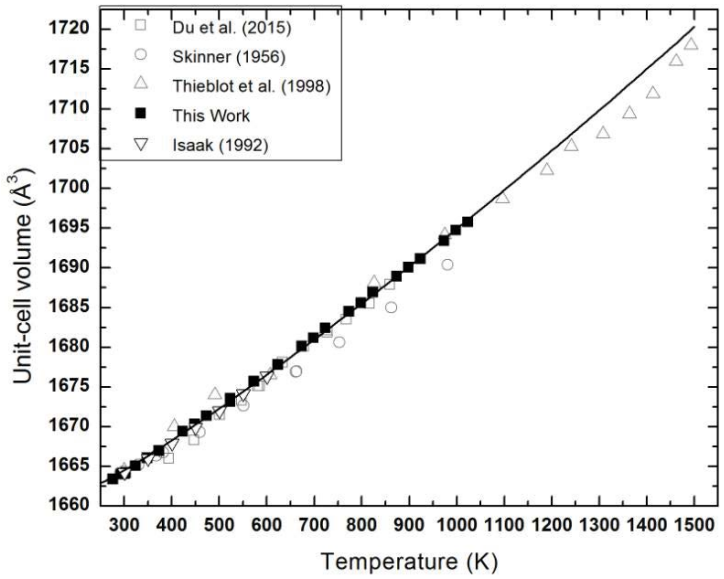

This is a preprint, the final version is subject to change, of the American Mineralogist (MSA)
Cite as Authors (Year) Title. American Mineralogist, in press.
DOI: https://doi.org/10.2138/am-2017-5855

Figure 2C

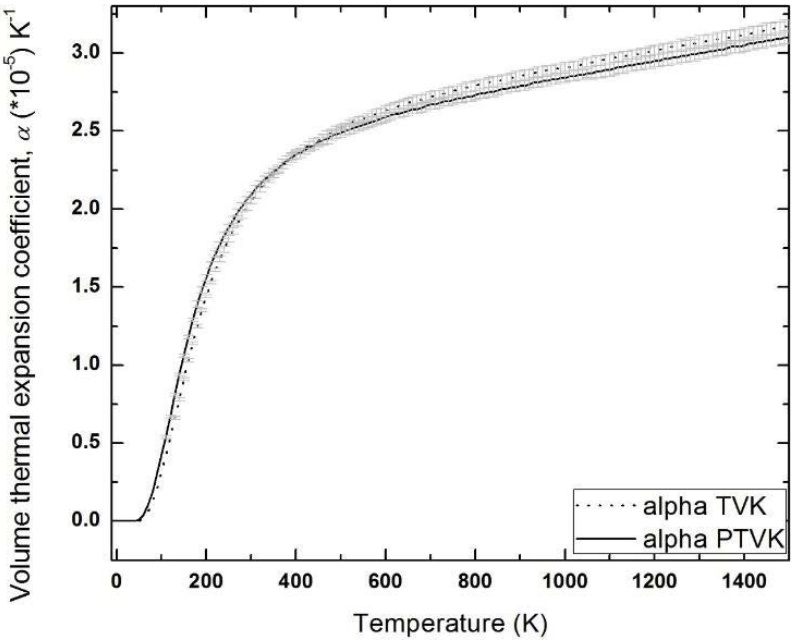

This is a preprint, the final version is subject to change, of the American Mineralogist (MSA)
Cite as Authors (Year) Title. American Mineralogist, in press.
DOI: https://doi.org/10.2138/am-2017-5855

Figure 3

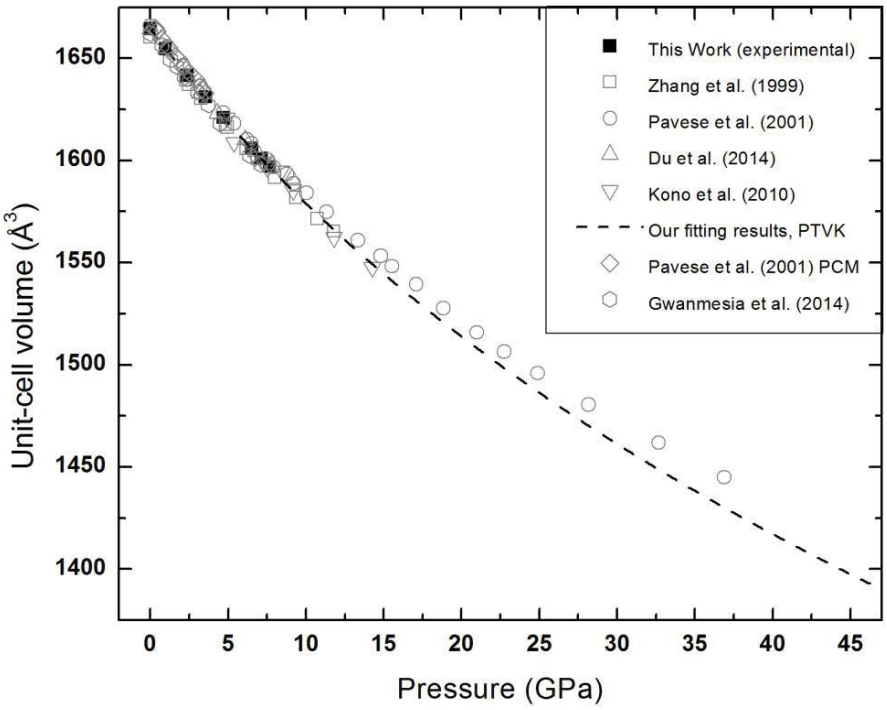

This is a preprint, the final version is subject to change, of the American Mineralogist (MSA)
Cite as Authors (Year) Title. American Mineralogist, in press.
DOI: https://doi.org/10.2138/am-2017-5855

Figure 4A

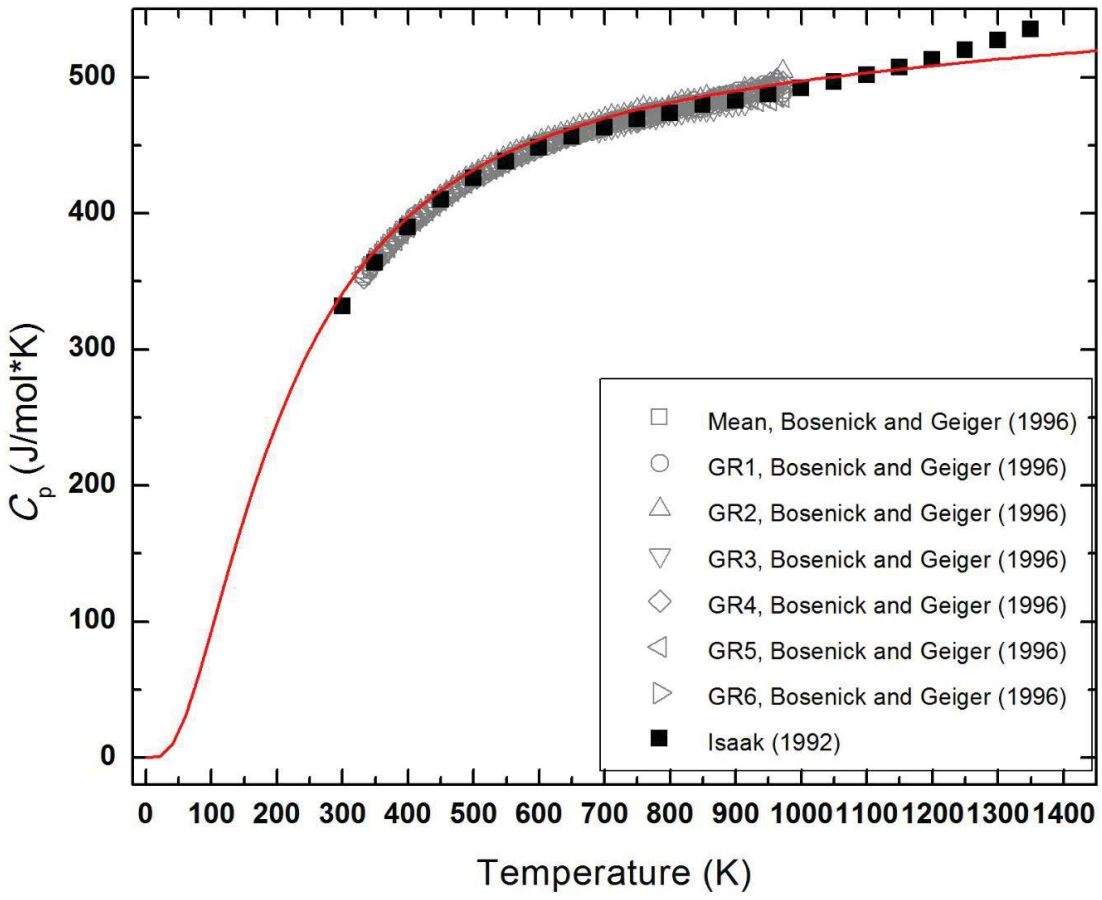

This is a preprint, the final version is subject to change, of the American Mineralogist (MSA)
Cite as Authors (Year) Title. American Mineralogist, in press.
DOI: https://doi.org/10.2138/am-2017-5855

Figure 4B

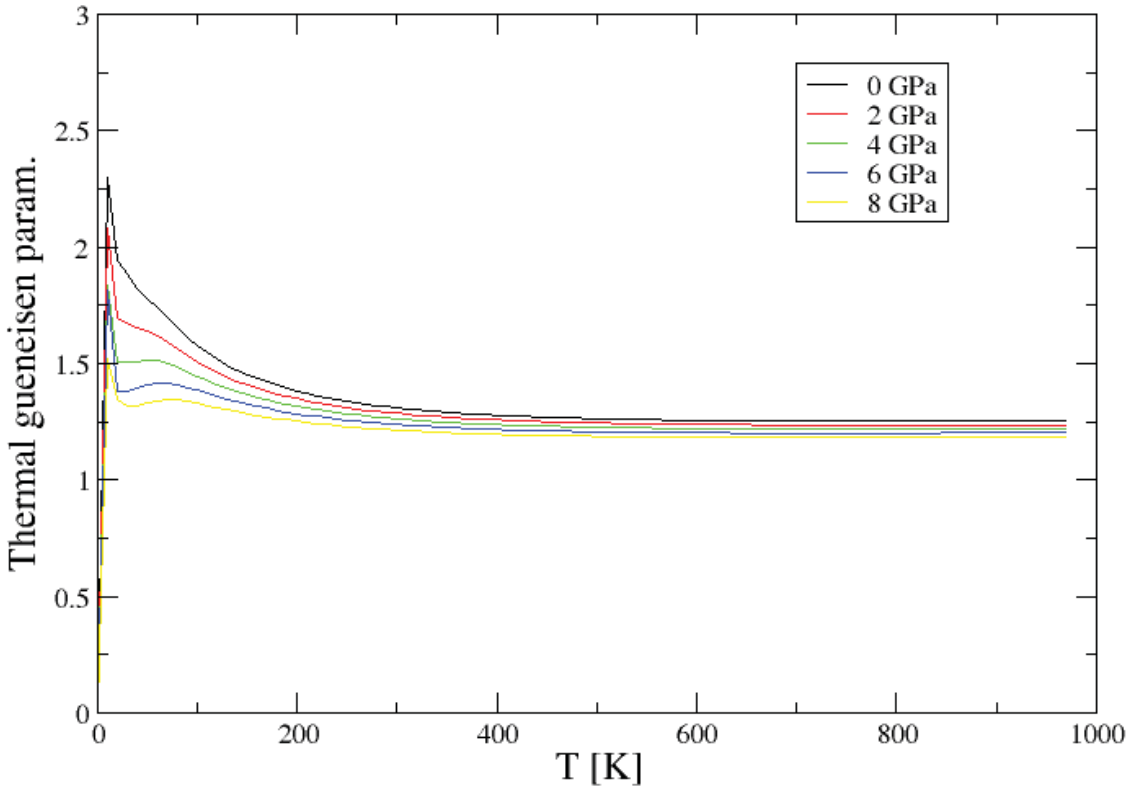

This is a preprint, the final version is subject to change, of the American Mineralogist (MSA)
Cite as Authors (Year) Title. American Mineralogist, in press.
DOI: https://doi.org/10.2138/am-2017-5855

Figure 5A

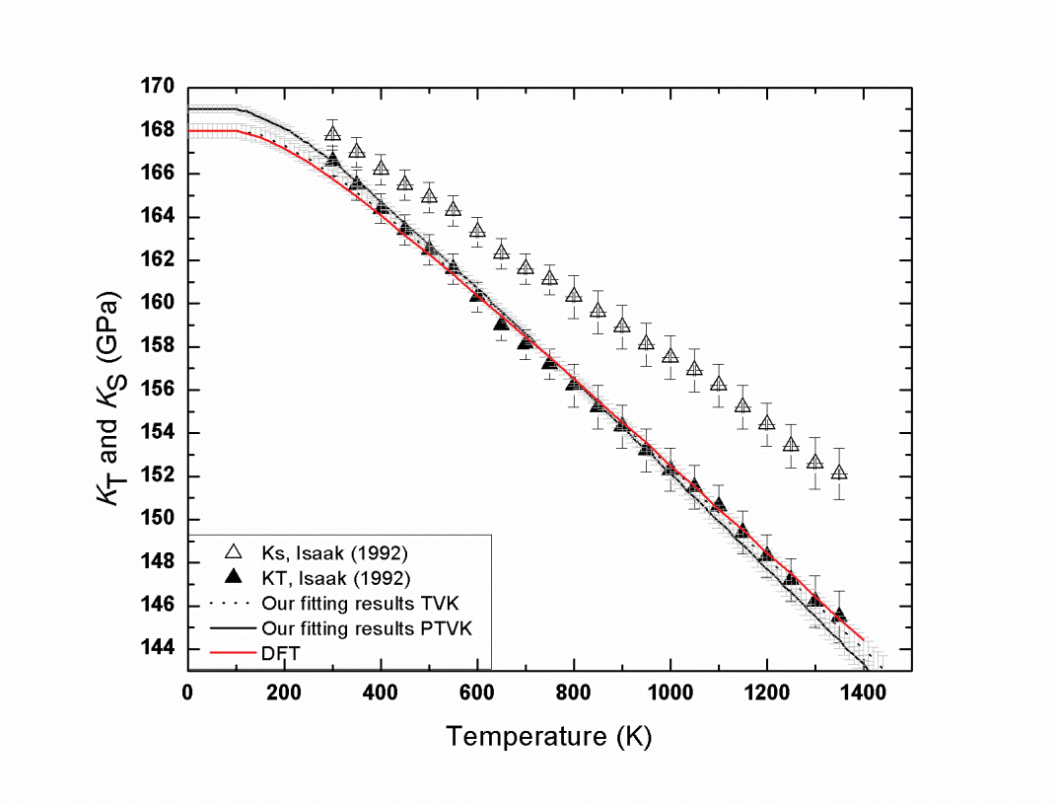

This is a preprint, the final version is subject to change, of the American Mineralogist (MSA)
Cite as Authors (Year) Title. American Mineralogist, in press.
DOI: https://doi.org/10.2138/am-2017-5855

Figure 5B

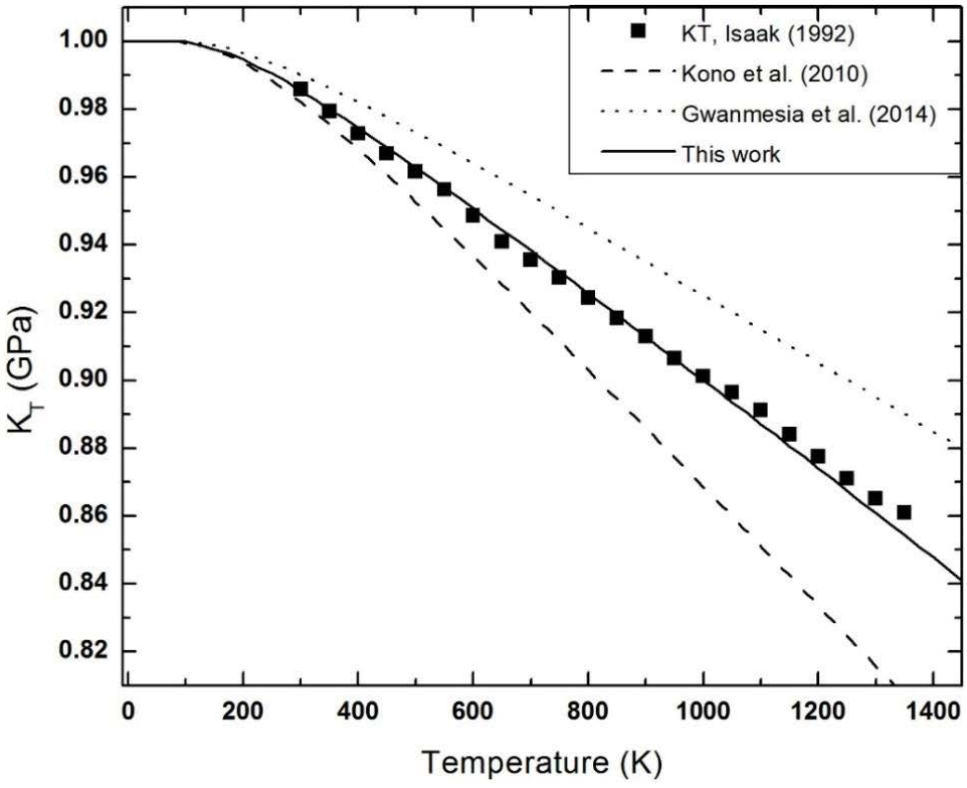

This is a preprint, the final version is subject to change, of the American Mineralogist (MSA)
Cite as Authors (Year) Title. American Mineralogist, in press.
DOI: https://doi.org/10.2138/am-2017-5855

Table 1 Averaged composition obtained from EMPA analyses on grossular synthetic single crystal garnets.

n. analyses		8	
	wt%		*a.p.f.u.*
SiO_2	40.13 (13)	Si	3.00(1)
Al_2O_3	22.33 (10)	Al	1.98(1)
CaO	37.83 (16)	Ca	3.04(1)
Total	100.32		8.01(1)

Standard deviations are given in parentheses.

This is a preprint, the final version is subject to change, of the American Mineralogist (MSA)
Cite as Authors (Year) Title. American Mineralogist, in press.
DOI: https://doi.org/10.2138/am-2017-5855

Table 2. Unit-cell edge and volume of grossular at different temperatures.

T (K)	a (Å)	V (Å^3)
100(2)	11.8403(13)	1659.92(33)
110(2)	11.8405(14)	1659.99(33)
120(2)	11.8407(13)	1660.10(32)
130(2)	11.841(13)	1660.20(33)
150(2)	11.8417(13)	1660.52(33)
170(2)	11.8425(14)	1660.84(34)
190(2)	11.8437(14)	1661.37(34)
210(2)	11.8446(14)	1661.75(34)
230(2)	11.8454(14)	1662.05(35)
276(2)	11.8485(15)	1663.36(37)
293(2)	11.8499(5)	1663.98(20)
301(2)	11.8500(12)	1664.01(29)
303(2)	11.8503(6)	1664.15(23)
323(2)	11.8525(6)	1665.04(25)
348(2)	11.8548(5)	1666.02(21)
373(2)	11.8570(6)	1666.95(24)
423(2)	11.8627(7)	1669.36(28)
448(2)	11.8648(5)	1670.26(22)
473(2)	11.8673(7)	1671.31(31)
523(2)	11.8716(12)	1673.12(49)
523(2)	11.8726(5)	1673.55(21)
573(2)	11.8776(6)	1675.65(26)
623(2)	11.8826(5)	1677.78(22)
673(2)	11.8880(5)	1680.08(22)
698(2)	11.8905(5)	1681.14(21)
723(2)	11.8934(5)	1682.38(23)
773(2)	11.8984(5)	1684.47(23)
798(2)	11.9009(5)	1685.53(22)
823(2)	11.9041(6)	1686.92(24)
873(2)	11.9088(6)	1688.90(25)
898(2)	11.9114(5)	1690.01(22)
923(2)	11.9139(5)	1691.09(23)
973(2)	11.9193(5)	1693.38(22)
998(2)	11.9224(5)	1694.69(21)
1023(2)	11.9248(5)	1695.71(22)

Note: Standard deviations are given in parentheses.

This is a preprint, the final version is subject to change, of the American Mineralogist (MSA)
Cite as Authors (Year) Title. American Mineralogist, in press.
DOI: https://doi.org/10.2138/am-2017-5855

Table 3. Unit-cell edge and volume at different pressures.

P (GPa)	a (Å)	V (Å^3)
0.0001(1)	11.8508(3)	1664.34(14)
1.013(9)	11.8275(4)	1654.55(15)
2.392(10)	11.7963(4)	1641.47(15)
3.568(10)	11.7712(3)	1631.04(13)
4.715(11)	11.7469(3)	1620.95(13)
6.559(15)	11.7101(4)	1605.76(15)
7.149(12)	11.6986(3)	1601.05(14)
7.674(19)	11.6886(5)	1596.95(19)

Standard deviations are given in parentheses.

This is a preprint, the final version is subject to change, of the American Mineralogist (MSA)
Cite as Authors (Year) Title. American Mineralogist, in press.
DOI: https://doi.org/10.2138/am-2017-5855

Table 4a. Literature bulk moduli for grossular compared to our experimental and theoretically calculated data.

	Expermental method	V_0 (Å^3)	K_{T0} (GPa)	K'	Pressure medium	P_{max}(GPa)	Synthesis Method
Isaak (1992)	RUS	-	166.4(0.7)	-	-	-	
Zhang et al., 1999	X-ray single crystal diffraction	1660.218(337)	170(4)	5.2(6)	Ne	11.8	synthesized hydrothermally at high pressure and temperature in a piston cylinder device (Armbruster et al., 1992)
Akhmatskaya et al., 1999	DFT^{GGA} (static)	1667.0	166(2)	4.26(11)	-	-	-
Nobes et al., 2000	DFT^{GGA} (static)	1666.96	166	4.3	-	100	-
Mittal et al., 2001	lattice dynamic calculation	1665.18	170.41	-	-	-	-
Kono et al., 2010	Ultrasonic wave velocity	-	170.3(8)	4.43(7)	MgO+NaCl sleves	17	Hot-pressed glass with grossular composition at ~7 GPa and ~1 673 K for 2 h using a 3 000-ton high-pressure apparatus
Kawai et al., 2012-	DFT^{LDA} (static)	-	176.5	4.43	-	30	-
Erba et al., 2014	hybrid DFT ^{B3LYP} (static)	-	169.3	-	-	-	-
Pavese et al. (2001)	Powder diffraction	1666.3(3)	168.2(1.7)	5.9(2)		37	Pressure calibrant NaCl
Du et al. (2014)	Synchrotron X-ray powder diffraction	1664.3(3)	163.4(1)	5.92*	4:1 mixture of methanol:ethanol		anhydrous glass starting material in a multi-anvil (MA) 6GPa and 1400±2°C for 0.5h
Gwanmesia et al. (2014)	transfer-function ultrasonic interferometry plus energy-		169.5(2)	4.47(1)			Polycrystals hot-pressed in a 2000-ton uniaxial split-sphere apparatus at 15 kbar and nominal temperature 1000–1040°C for

This is a preprint, the final version is subject to change, of the American Mineralogist (MSA)
Cite as Authors (Year) Title. American Mineralogist, in press.
DOI: https://doi.org/10.2138/am-2017-5855

	dispersive synchrotron X-ray in MA apparatus						7 h.
This study	X-ray single crystal diffraction	1664.36(7)	167.45(1.04)	4.93(31)	methanol:ethanol (4 : 1)	7.7	Oxide mixture at 6 GPa and 1300°C in a multi-anvil press
	DFT^{PBEsol} (static)	1664.5	162.7	4.58		10	
	$DFT^{PBEsol+QHA}$ (ZPE)	1681.9	159.8	4.2		10	
	$DFT^{PBEsol+QHA}$ (300K)	1687.7	156.3	4.2		10	

Note: * value not refined

This is a preprint, the final version is subject to change, of the American Mineralogist (MSA)
Cite as Authors (Year) Title. American Mineralogist, in press.
DOI: https://doi.org/10.2138/am-2017-5855

Table 4b. Thermal expansion behaviour of the grossular garnet fitted by a Fei-type EoS at 300 K.

$V_{303\ K}$ calculated (Å^3)	$\alpha_{298K,1bar}$ x10^{-5} (K^{-1})	a_0 x10^5 (K^{-1})	a_1 x10^{10} (K^{-2})	a_2 (K)	EoS formalism	Reference
1664.2(1)	2.3(3)	2.84(32)	-0.2(3)	-0.4(3)		This work
1664.3(1)	1.7(4)	1.9(5)	0.8(5)	-0.4(4)	Fei-type[4]	Skinner (1956)[1]
1505.2(9)	1.7(6)	2.5(6)	30(50)	-0.9(10)		Thieblot et al. (1998)[2]
1664.3(3)	0.7(1.7)	6.60(18)	-4(2)	-4.1(15)		Du et al. (2015)[3]
1664.45(7)	2.08(2)[5]				Kroll-type	This work[6]

Note: [1]data have been fitted to the entire range of temperature (284 K to 980 K); [2]data have been fitted to the range of temperature between 300K-1453K not considering 3 outliers; [3] data have been fitted to the entire temperature range (296 K – 859 K) excluding two outliers. [4]Fei-type coefficients reported are calculated using as T_{ref} the first experimental temperature collected for each dataset; [5]θ_E=515(20) has been refined during fit; [6]EoS coefficients file (.eos) readable from EoSFit7c has been deposited as a supplementary material and is also available from the authors.

This is a preprint, the final version is subject to change, of the American Mineralogist (MSA)
Cite as Authors (Year) Title. American Mineralogist, in press.
DOI: https://doi.org/10.2138/am-2017-5855

Table 4c. Equation of State (EoS) cofficients obtained from simultaneous fitting of the P-V-T-K data. For all the datasets here reported a themal pressure EoS has been combined to a 3rd order Tait EoS.

Fitting type	V_0 (Å^3)	K_{T0} (GPa)	K'	α	θ_E	Reference
T-V-K^S	1664.18(3)	166.0(3)	4.73(15)	2.043(19)	567(13)	This study
T-V-K^T	1664.18(3)	166.0(3)	4.60(14)	2.043(19)	569(13)	This study
P-V-T-K^T	1664.46(5)	166.57(17)	4.96(7)	2.09(2)	512(19)	This study
P-V-T	1664.44(6)	166.1(1.1)	5.2(3)	2.09(2)	512*	
P-V-T-K^T	1667(6)	153(24)	6(3)	2.2(4)	512*	Kono et al (2010)
P-V-T-K^T	1658.3(1.0)	167(2)	4.8(4)	1.58(13)	512*	Gwanmesia et al (2014)

Note: *Value fixed in the refinement; γ and q values fixed as described in the text.